Journal of Hydrology 512 (2014) 39–52

Contents lists available at ScienceDirect

Journal of Hydrology

journal homepage: www.elsevier.com/locate/jhydrol

Mapping shallow lakes in a large South American floodplain: A frequency approach on multitemporal Landsat TM/ETM data

Marta Borro [a], Natalia Morandeira [a], Mercedes Salvia [b], Priscilla Minotti [a], Pablo Perna [b], Patricia Kandus [a,*]

[a] Laboratorio de Ecología, Teledetección y Eco-informática, Instituto de Investigación e Ingeniería Ambiental, Universidad Nacional de San Martín, Av. 25 de Mayo y Francia, B1650HMP General San Martín, San Martín, Provincia de Buenos Aires, Argentina

[b] Grupo de Teledetección Cuantitativa, Instituto de Astronomía y Física del Espacio (UBA-CONICET), Intendente Güiraldes 2160, 1428 Ciudad Autónoma de Buenos Aires, Argentina

ARTICLE INFO

Article history:
Received 5 April 2013
Received in revised form 21 January 2014
Accepted 22 February 2014
Available online 3 March 2014
This manuscript was handled by Konstantine P. Georgakakos, Editor-in-Chief, with the assistance of Marco Borga, Associate Editor

Keywords:
Shallow lakes map
Paraná River floodplain
Wetlands
Multitemporal frequency approach
Landsat time series

SUMMARY

We propose a methodology to identify and map shallow lakes (SL) in the Paraná River floodplain, the largest freshwater wetland ecosystem in temperate South America. The presence and number of SL offer various ecosystem services and habitats for wildlife biodiversity. Our approach involved a frequency analysis over a 1987–2010 time series of the Normalized Difference Vegetation Index (NDVI), derived from Landsat 5 and 7 TM/ETM data. Through descriptive statistics of samples of pixels and field work in different types of SL, we established an NDVI threshold of 0.34 below which we assumed the presence of water in each pixel. The standard deviation of the estimated SL area decreases with the number of images in the analysis, being less than 10% when at least 30 images are used. The mean SL area for the whole period was 112,691 ha (10.9% of the study area). The influence of the hydrological conditions on the resulting SL map was evaluated by analyzing twelve sets of images, which were selected to span the whole period and different time frames according to multiannual dry and wet periods and to relative water level within each period. The Kappa index was then calculated between pairs of resulting SL maps. We compared our maps with the available national and international cartographic documents and with other published maps that used one or a few Landsat images. Landsat images time series provide an accurate spatial and temporal resolution for SL identification in floodplains, particularly in temperate zones with a good provision of cloud free images. The method evaluated in this paper considers the dynamics of SL and reduces the uncertainties of the fuzzy boundaries. Thus, it provides a robust database of SL and its temporal behavior to establish future monitoring programs based on the recent launch of Landsat 8 satellite.

1. Introduction

The largest freshwater wetlands of South America are associated with the floodplains of large rivers such as the Amazonas, the Orinoco and the Paraná (Neiff, 1990; Iriondo, 1988). These wetlands present spatio-temporal hydrological fluctuations, mainly due to annual phases of flood and drought pulses (Junk et al., 1989). Fluctuations of the water table constrain biogeochemical cycles and fluxes, promote soils with strong hydromorphic features and support a very rich biota well adapted to a wide range of water availability and hydroperiods (Neiff et al., 1994; Keddy, 2010). One of the distinctive feature of floodplains is the presence and number of shallow lakes (SL), which provide several ecological services such as the supply of nursery areas for commercial fish, toad and tadpole habitats, cattle grazing, bee flora and floods regulation (Quirós and Cuch, 1989; Poi de Neiff and Neiff, 2006; Sendacz, 2001; Bó and Quintana, 1999; Baigún et al., 2008). At landscape scale, flood and drought pulses usually change the connectivity between shallow lakes and lotic water bodies (river and streams channels). In addition, the complex dynamic between vegetated and water-covered sites drives the exchange of sediments, organic matter and organisms between the floodplain matrix (usually vegetated) and the SL and lotic water bodies. As a consequence, both the boundaries and the area of SL may be variable in wetland ecosystems. SL, the water bodies that dominate many temperate floodplains, are specially affected by these hydrological fluctuations and landscape scale dynamics (Junk et al., 1989).

Shallow lakes are lentic water bodies with neither vertical stratification nor barriers to the transport of solutes and materials (Padisák and Reynolds, 2003). Pragmatic definitions of SL have established a maximum depth of 3 m (Scheffer, 1998) or 5 m (Padisák and Reynolds, 2003). However, the maximum depth of a

* Corresponding author. Tel./fax: +54 11 4006 1500x6037.
E-mail addresses: marta.borro@gmail.com (M. Borro), nmorandeira@unsam.edu.ar (N. Morandeira), msalvia@iafe.uba.ar (M. Salvia), pminotti@unsam.edu.ar (P. Minotti), pperna@iafe.uba.ar (P. Perna), pkandus@unsam.edu.ar (P. Kandus).

http://dx.doi.org/10.1016/j.jhydrol.2014.02.057
0022-1694/

SL depends on the water body area, its position in the landscape and also on how the wind affects the water body. Sedimentation–resuspension processes, heat content variations and general thermal behavior of SL are closely linked to flood and drought pulses driven by the floodplain hydrology (Drago, 2007; Neiff, 1990; Junk et al., 1989). Despite the ecological importance of SL, studies of their distribution in wetlands floodplains are scarce (Cózar et al., 2005; Mertes et al., 1996; Cowardin and Peterson, 1997; Silva et al., 2008) and their spatio-temporal dynamics have often been ignored (Stein, 2008). Indeed, knowing the distribution of the SL is critical to better understanding of the floodplain dynamics, to monitor wetland ecosystems and also to assess habitat for wildlife species (De Jager and Rohweder, 2012).

An accurate way to account for this issue is to elaborate maps of SL via remote sensing data processing, but this is not a straightforward process. SL are usually fragmented, have intrinsic spatial and temporal variability and are often partially or totally covered by vegetation, especially in the floodplains of large rivers. Thus, SL boundaries appear as a set of mixed pixels in satellite images, which contributes to uncertainties about their areal extent (Ozesmi and Bauer, 2002). Besides, annual and interannual hydrological pulses promote cyclic changes in water cover types, usually described as lake stages (Scheffer, 1998). Major water cover types are water with emergent macrophyte communities, open water with high inorganic turbidity, clear open water and green turbid water. Even a smooth relief can mark a transition between dense vegetation with saturated soil, sparsely distributed plants with shallow and turbid standing waters, and deep open waters. Therefore, wide transition zones between marshes and open water need to be considered to extract SL areas from satellite images.

Open water can be easily distinguished from vegetation due to its characteristic spectral signature, usually condensed in spectral feature spaces (Ozesmi and Bauer, 2002). However, the use of only one image of a single date may lead to misclassification of other SL cover types and to artificially imposed SL boundaries. True boundaries between a SL and its surroundings may have several spectral signatures widely spread in spectral feature spaces, including mixtures of shallow water, wet soil, flood debris, dead flattened algae and sparsely distributed young flush sedges (Zhao et al., 2011). These signatures might also overlap with those of the surrounding vegetation of drier environments. Thus, accurate mapping of SL requires the detection of spatio-temporal variability and landscape scale changes due to annual and interannual hydrological fluctuations.

A widespread way to capture spatio-temporal variability into a map is through the use of multitemporal data sets of optical imagery (Olmanson et al., 2008). Several satellite indices have been developed and used in multitemporal analysis. However, most of them were developed for different aspects of vegetation monitoring purposes. Some of them, like NDWI (Gao, 1996) or NDII (Hardisky et al., 1983), were designed to monitor vegetation water content using infrared reflectance. The Wetness band from Tasseled cap transformation (Crist and Cicone, 1984) was developed to enhance the presence of water, but cannot distinguish by itself between vegetation water content, soil moisture or water body presence. On the other hand, although the Normalized Difference Vegetation Index (NDVI) (Tucker, 1979) has been developed for vegetation status monitoring purposes, it can discriminate water bodies from bare soil and vegetation due to the use of the "red edge" (NIR and red reflectance difference): water has larger reflectance in red than in NIR wavelengths, soil has similar reflectance at both red and NIR wavelengths, and vegetation has larger reflectance in red than in NIR. In addition, NDVI is one of the most commonly used index for temporal comparisons. The results achieved with Landsat can be easily compared with results obtained with other sensors and between geographic areas due to the large documentation available about its behavior in different environmental conditions (Weiss and Crabtree, 2011; Caccamo et al., 2011). Nowadays, since the NDVI standard products from "AVHRR" and "MODIS" sensors are widely available, comparing results at different scales is also interesting.

Moderate spatial resolution imagery with high temporal resolution (i.e., the generated by MODIS sensors) may offer useful data set to delineate wetlands, but have low spatial resolution (Peng et al., 2005; Feng et al., 2012). Indeed, the Landsat TM/ETM system has higher spatial resolution than MODIS, combined with good coverage and data availability along a 27-year period (Kloiber et al., 2002; Ritchie et al., 2003).

The aim of this study was to identify and map the SL of the Lower Paraná River floodplain. The approach involved a frequency analysis over a two decade time series of the Normalized Difference Vegetation Index (NDVI), derived from Landsat Thematic Mapper (TM) and Enhanced Thematic Mapper (ETM) data. We also aimed to evaluate the effect of the number of images used in the analysis and of the pluriannual hydrological conditions on the resulting SL map. Finally, we compared our map with the available national and international cartographic documents and with other maps that have been obtained by other authors with the use of only one or a few Landsat images of the study area.

2. Material and methods

2.1. Study area

The study was carried out in the Lower Paraná River floodplain, which is a temperate freshwater wetland. The study area is placed in the upper and middle portions of the Paraná River Delta region and covers 1,033,313 ha between 60°35′29″ W, 32°20′45″ S and 59°51′37″ W, 33°31′ S, next to Victoria, Rosario and San Pedro cities of Argentina (Fig. 1). The Paraná River flows from tropical latitudes to temperate zones and joins the Uruguay River at the Del Plata estuary. The Paraná River average water discharge can range from 16,000 m^3/s to 60,000 m^3/s, ranking second in South America (after the Amazon River) in terms of basin size and length (Neiff et al., 1994; Latrubesse et al., 2005). The Lower Paraná River floodplain (also known as the Paraná Delta region) is a coastal-fluvial complex developed during the last 6000 years (Iriondo and Scotta, 1979). The current hydrological regime is dominated by floods from the Paraná River. The flood pulse of the Paraná River is more irregular than those of larger South American rivers such as the Amazonas or the Orinoco (Carignan and Neiff, 1992). The main peak of the flood pulse in this area occurs at the end of the summer (March) and is caused by the hydrology of the Upper Paraná River. A second peak takes place during the winter (June–July) from the Paraguay River. The lowest levels of the Lower Paraná River in the study area are typical during the change from cold to warm season (September). During strong El Niño events, extended floods affect the whole study area. Additionally, the alternation of relatively wet and dry decades provides an extra source of variability (Fig. 2).

The landscape of the Lower Paraná River floodplain is a complex mosaic of marshes, which is dotted with a large number of shallow lakes. The dominant vegetation types are broadleaf herbs (i.e., *Polygonum* spp., *Ludwigia elegans*, *Alternanthera philoxeroides*, *Eichhornia* spp.), tall graminoids (i.e., *Hymenachne* spp., *Panicum elephantipes*, *Coleataenia prionitis*), medium graminoids (*Echinochloa* spp., *Bromus catharticus*), short graminoids (height < 0.5 m) (*Cynodon dactylon*, *Luziola peruviana*, *Leersia hexandra*, *Paspalum vaginatum*) and equisetoids (*Schoenoplectus californicus*, *Cyperus giganteus*) (Morandeira et al., 2011; Kandus et al., 2003; Malvárez, 1997; Quintana et al., 2005). SL are spread in this marsh mosaic and appear and disappear according to water table level and flood

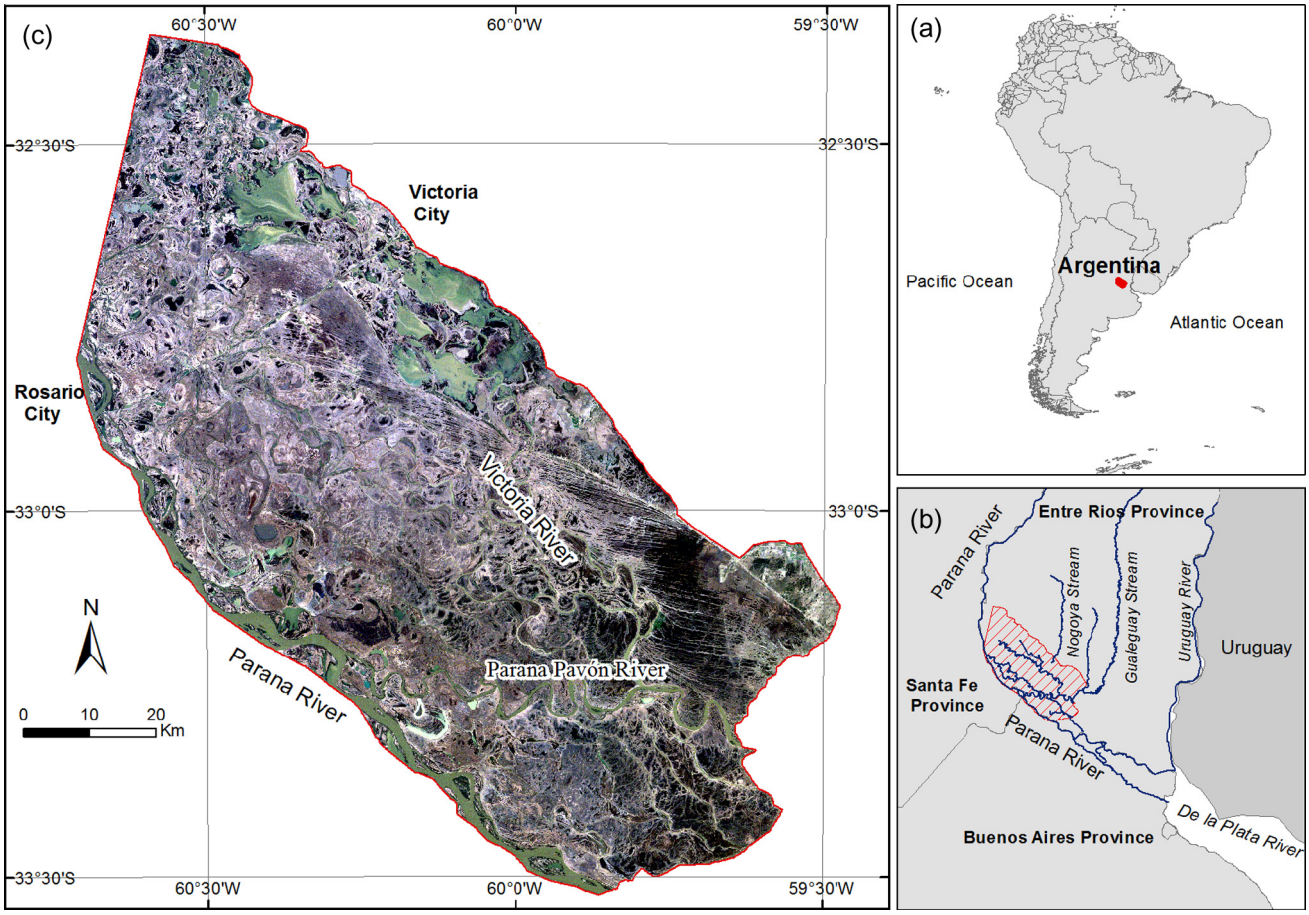

Fig. 1. Location of the study area in (a) South America, (b) Argentina and (c) subset of Landsat 5 TM image of 6 August 2009 displayed in "Real Color" layer combination (RGB: Red = Band 3, Green = Band 2, Blue = Band 1). The main cities and rivers are shown. (For interpretation of the references to colour in this figure legend, the reader is referred to the web version of this article.)

and drought pulses, constantly changing shape, size and cover type.

2.2. Images sources and pre-processing

We used 77 Landsat images (68 Landsat 5 TM and 9 Landsat 7 ETM+), Path/Row 226/83, provided by CONAE (Comisión Nacional de Actividades Espaciales, Argentina). These were the only cloud free images available from the 526 scenes that the Landsat sensor could have potentially acquired every 16 days, for the study area from 1987 to 2010 (23 years). In the case of Landsat 7 ETM + we used images before May 2003 when Scan Line Corrector (SLC) was damaged (Fig. 2a). The coefficient of variation (CV = SD/mean) was calculated for the number of days between successive images. The result was 115.3/109.5 = 1.05. A CV close to one indicates a random distribution, lower than one, regular, and higher than one, agregated.

We performed image geometric corrections with a first order polynomial transformation and nearest neighbor resampling method, with a root square of less than 0.5 pixels. Digital numbers were transformed into surface reflectance assuming that the influence of the atmosphere can be modeled by considering the additive effect of Rayleigh dispersion (Stumpf, 1992).

2.3. NDVI thresholding for shallow lakes water identification

In order to discriminate shallow lake water from surrounding vegetated wetlands on a single date, we used the Normalized Difference Vegetation Index – NDVI (Tucker, 1979) as an indicator of both vegetation and water coverage.

The NDVI values range from −1 to 1: high positive values correspond to closed plant coverage, low positive values to areas with sparse plant coverage, zero values to predominance of bare soil and negative values to water (Tucker, 1979). Regarding SL, we expect negative values when open water is present, with increasing and even positive values when the proportion of plant coverage over water increases.

A NDVI threshold value (T) was used to classify each NDVI image in two classes according to the presence or absence of SL. The threshold was established by analyzing the mean values and dispersion of the NDVI pixels from 26 samples of different land cover types. The land cover types that dominate the study area were assessed with field work at dates close to the dates of the used Landsat TM images (December 25th 2008, October 12nd 2010 and January 1st 2011). SL include the following land cover types: water bodies with high content of suspended sediments, water bodies with high content of phytoplankton, water bodies only with submerged macrophytes, clear water bodies with emergent macrophytes (mainly as boundary vegetation), and water bodies fully covered with emergent and floating macrophytes; whereas SL absence was associated to marshlands fully covered with herbaceous plant communities.

We calculated the mean NDVI values of each of the land cover types and tested if significant differences existed between the land cover types associated with SL presence and SL absence. This was done using a t-test with a Welch–Satterthwaite approximation to

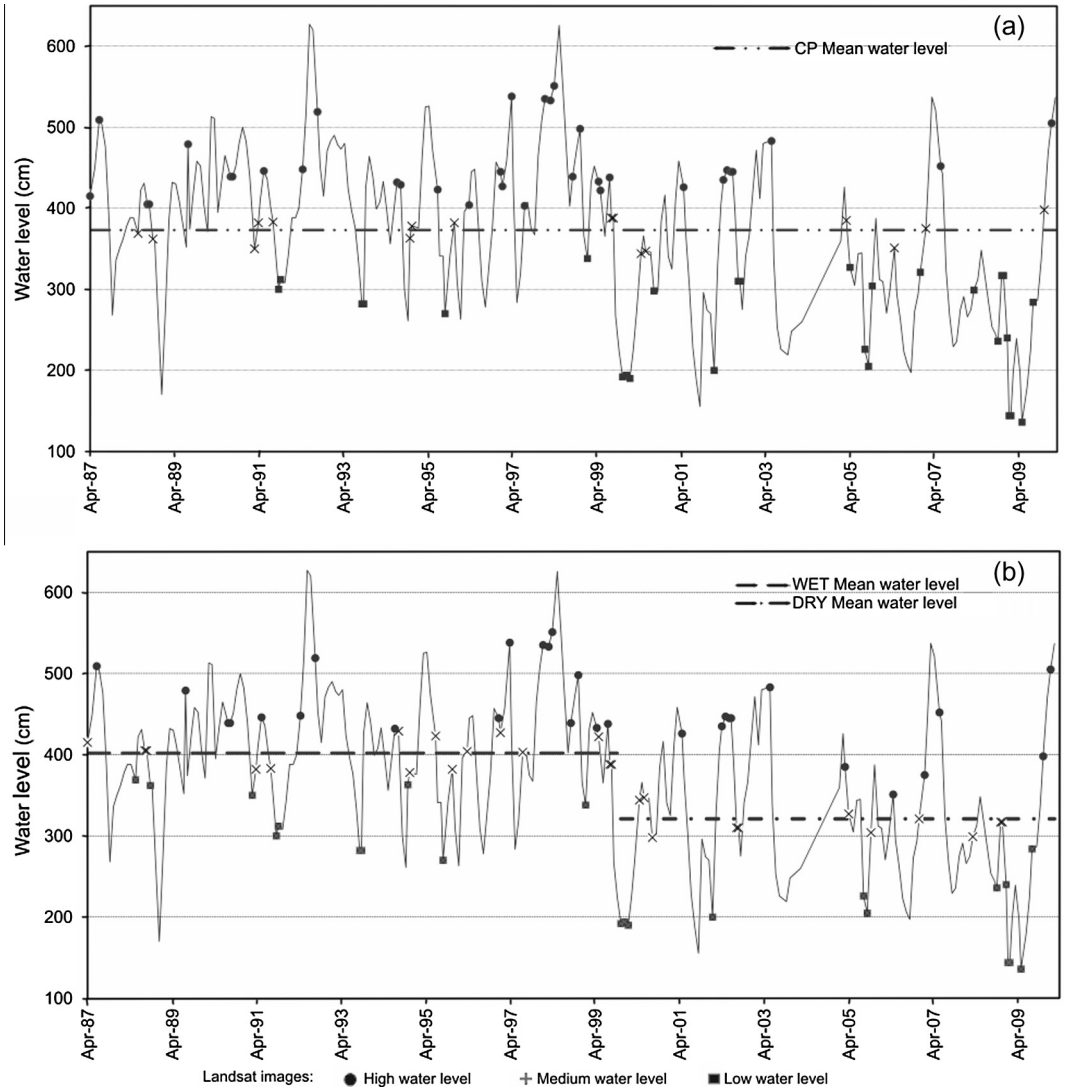

Fig. 2. Monthly mean water level measured from 1987 to 2010 at the Paraná River next to Rosario. (a) Complete period 1987–2010, (b) WET period 1987–1999, DRY period 1999–2010. Dates of Landsat images used are marked. Source of water level records: Prefectura Naval Argentina (http://www.prefecturanaval.gov.ar/web/es/html/dico_alturas.php).

the degrees of freedom (Satterhwaite, 1941) (i.e., a modification of the Student t-test intended for use with two samples having possibly unequal variances). The statistical analyses were performed with R (R Core Team, 2012). Having significant differences, we selected as threshold (T), the maximum value of the mean NDVI reached by the land covers associated with SL.

A binary shallow water (BSW) layer was obtained from each of the 77 NDVI masked images by segmenting into values equal or less than the estimated threshold: if a pixel was below the threshold (T), it was set to 1; otherwise, it had value 0. In each BSW layer, pixels with the value 1 include shallow lakes and areas that were flooded at that date.

2.4. Multitemporal shallow lake mapping

2.4.1. Aboveground water presence frequency layer

With a highly variable hydrology, a single image cannot adequately represent the extent of shallow lakes, so we used a frequency approach to estimate the aboveground water presence frequency at each pixel in a given set of images s (see below, Section 2.5):

$$\mathrm{AWPF}_{sj} = \frac{\sum_{i=1}^{Ns} BSW_{ij}}{N_s} \quad (1)$$

where AWPF_{sj} is the aboveground water presence frequency value of the pixel j for the set s and represents the proportion of images i with BSW equal to 1 in the pixel j (BSW_{ij}) in relation to the total number of images in the analyzed set of images (N_s). Thus, a pixel j that was equal to 1 in every BSW layer of the set s had a value of 1 in the resulting AWPFs layer (the pixel was always with water aboveground), whereas a pixel that was equal to 0 in every BSW layer of the set s had a value of 0 in the resulting AWPFs layer.

We made a sub-scene of the study area by separating image pixels corresponding to the floodplain from the uplands. In order to avoid confusion in the quantification of pixels of shallow lakes, we masked the rivers and streams. For this task, we used the thematic layer (water bodies and streams) of SIG250 which is the only national (Argentinean) standard cartography available for the whole country (227 sheets at 1:250,000 scale) referenced in geographic coordinates in the WGS 84 reference frame POSGAR 94. Note that the national cartography is named SIG250 (Instituto Geográfico Nacional, 2001) due to the scale and not due to the pixel

size. Indeed, the cartography is updated with basis on Landsat images (30 m of pixel size) and thus is adequate for our purpose.

2.4.2. Shallow lake map

Each of the AWP*Fs* layers was transformed into a SL map by segmenting it into four shallow lake water frequency classes which describe the degree of water permanence in each pixel: permanently with water ($0.8 \geqslant AWPF_{sj} \geqslant 1$), usually with water ($0.6 \geqslant AWPF_{sj} > 0.8$), regularly with water ($0.4 \geqslant AWPF_{sj} > 0.6$), occasionally with water ($0 \geqslant AWPF_{sj} > 0.4$). Pixels classified as "occasionally with water" may be areas which are seldom flooded or areas covered by such dense vegetation that water cannot be detected in most of the images. We considered that a pixel is SL in the set *s* if it is waterlogged at least regularly ($AWPF_{sj} \geqslant 0.4$).

2.5. Minimum number of scenes needed for shallow lake mapping

We carried out a sensitivity analysis to assess whether the SL area differed with the number of dates used and to define the optimum number of images needed in the analysis. The SL area was estimated in sets of 5, 10, 15, 20, 25 and 30 randomly chosen BSW layers, with 20 repetitions for each set size. Differences between the estimated SL areas for the sets sizes were carried out by means of a Kruskal Wallis test (followed by pair comparisons) because no normal distribution was found for SL area or its logarithmic, square-root or quadratic transformations. The variation of the percentage of standard deviation with the number of images used was described with a linear regression model. The optimum number of images needed in the following steps of the analysis was the lower number of images with a standard deviation of the SL area less than 10%. When less than the optimum number of images was used, the standard deviation of the resulting SL area was estimated with the linear regression model. The statistical analyses were performed with R (R Core Team, 2012).

2.6. Available hydrological scenarios

To assess the temporal variability of the SL distribution, we built BSW sets representing different hydrological situations. Taking into account multiannual variations, we identified three contrasting situations based on overall mean water level of Rosario city Paraná River gauge station (Prefectura Naval Argentina):

2.6.1. Complete period (CP)

Included the 77 BSW layers of the complete period analyzed in this study (1987–2010) (Fig. 2a).

2.6.2. High water level period (WET)

Included 42 BSW layers of a high water level period (1987–1999) (Fig. 2b).

2.6.3. Low water level period (DRY)

Included 35 BSW layers from a low water level period (2000–2010) (Fig. 2c).

For each period four BSW sets representing relative water level conditions, were compiled considering its mean water level: the complete set (Total); a low water set (LWL) which included scenes where water level was at least 30 cm below the water mean; a high water set (HWL) with scenes having levels higher than 30 cm above the mean; and a middle water set (MWL) where levels varied ± 30 cm around the period's mean (Table 2).

These sets of layers represent different hydrological scenarios (3 periods × 4 relative water level condition). For each of the 12 BSW sets a AWP*Fs* layer was calculated following Eq. (2), and a SLs map was obtained after frequency segmentation.

Table 1
List of the Landsat images used (Path/Row: 226/83) and the hydrological condition of the acquisition dates registered at the Rosario Port gauge. Source of water level records: Prefectura Naval Argentina (http://www.prefecturanaval.gov.ar/web/es/html/dico_alturas.php). Images were provided by National Aeronautics and Space Administration (NASA) through Comisión Nacional de Actividades Espaciales (CONAE, http://www.conae.gov.ar).

Image date	Water level (cm)
1/13/2010	543
11/10/2009	379
8/6/2009	265
5/2/2009	174
1/26/2009	160
1/10/2009	126
12/25/2008	196
11/23/2008	332
11/7/2008	300
10/6/2008	184
3/12/2008	303
5/29/2007	445
1/21/2007	375
12/4/2006	315
4/24/2006	351
10/14/2005	304
9/12/2005	205
8/11/2005	226
4/5/2005	295
3/4/2005	385
5/26/2003	483
8/27/2002	290
8/11/2002	316
6/24/2002	440
6/8/2002	452
5/7/2002	462
4/5/2002	406
1/15/2002	193
4/26/2001	401
8/13/2000	306
6/2/2000	380
4/23/2000	360
1/18/2000	180
12/17/1999	192
11/15/1999	190
8/27/1999	333
8/11/1999	420
7/26/1999	461
5/7/1999	443
4/21/1999	425
1/15/1999	323
11/12/1998	498
9/9/1998	439
4/2/1998	551
3/1/1998	533
1/12/1998	535
7/20/1997	403
3/30/1997	538
1/9/1997	427
12/24/1996	445
3/27/1996	404
11/20/1995	382
9/1/1995	270
6/29/1995	380
11/17/1994	363
11/1/1994	363
8/13/1994	429
7/12/1994	432
9/27/1993	282
9/11/1993	282
8/23/1992	519
4/17/1992	448
10/8/1991	312
9/22/1991	300
8/5/1991	383
5/17/1991	446
3/30/1991	382
2/26/1991	350

(*continued on next page*)

Table 1 (*continued*)

Image date	Water level (cm)
8/18/1990	439
8/2/1990	439
7/30/1989	352
9/29/1988	362
8/28/1988	405
8/12/1988	405
5/24/1988	369
6/23/1987	509
4/4/1987	415

Results obtained under different scenarios were compared in terms of total shallow lake water area and water frequency classes. Overall Kappa index (Congalton and Green, 1999) was used to assess the agreement of all the possible pairs of *SLs* maps based on the calculation of contingency matrices and extracting the contribution provided by random. Overall Kappa index (K) can be expressed as:

$$K = \frac{P_{(a)} - P_{(e)}}{1 - P_{(e)}} \quad (2)$$

where $P_{(a)}$ is the proportion of pixels that show agreement between the two maps compared and $P_{(e)}$ is the hypothetical probability of agreement only by chance. If the two maps compared are exactly the same, $P_{(a)} = 1$, and $K = 1$. If there is only agreement by chance, $P_{(a)} = P_{(e)}$, and $K = 0$. If there is no coincidence, $P_{(a)} = 0$ and $K < 0$.

The Kappa index is calculated as:

$$K = \frac{N\sum_{i=1}^{r} X_{ii} - \sum_{i=1}^{r} X_{i+} * X_{+i}}{N^2 - \sum_{i=1}^{r} X_{i+} * X_{+i}} \quad (3)$$

where r is the number of rows (classes in the map a), and also the number of columns (classes in map b); X_{ii} is the number of pixels corresponding to the row i and column i (pixels that show agreement between the two maps compared), X_{i+} and X_{+i} are the totals of each row and column respectively, and N is the total number of pixels in each of the maps.

We compared pairs of BSW maps, each of them with two classes (SL and Not SL). To evaluate the strength of agreement between two maps, we used the standards proposed by Landis and Koch (1977) for the Kappa coefficient: 0 = poor agreement, 1–20 = slight agreement, 21–40 = fair agreement, 41–60 = moderate agreement, 61–80 = substantial agreement and 81–100 = almost perfect agreement.

A flowchart showing the methodological steps is depicted in Fig. 3.

2.7. Comparison with published documents

The *SLs* maps were also compared with available published maps for the same study area (Borro et al., 2010a,b), with the national cartographic document SIG250 (Instituto Geográfico Nacional, 2001) and with the international Water Body data layer. The International Water Body was derived from data produced by the SRTM – Shuttle Radar Topography Mission that flew on board the Space Shuttle Endevour during an 11-day mission in February of 2000 (Rabus et al., 2003). The SRTM Water Body Data vector files are a by-product of the SRTM elevation data (90 m of spatial resolution) editing, performed by the National Geospatial-Intelligence Agency (NGA). Water bodies that meet minimum capture criteria (oceans, lakes and river shorelines) are identified and delineated. Overall and conditional Kappa indexes were calculated (Congalton and Green, 1999) (see Section 2.6). The previous maps were set as the reference in each of the comparisons. Comparisons with the maps built for the same study area were made considering similar hydrological conditions between the scenes used. In this way, the SLs map derived from DRY-LWL set were compared with that of Borro et al. (2010a) made by using a single Landsat image from August 8, 2009; the SLs map made derived from the complete set of images (CP-Total) was compared with the map of Borro et al. (2010b) built with an unsupervised classification of the minimum NDVI values of a multitemporal dataset of 34 Landsat5 TM and Landsat 7 + ETM randomly chosen images from 1987 to 2010. The twelve SLs maps obtained were compared to available lakes maps: lakes layer from SIG 250 and the SRTM Water Body Data.

Apart from overall Kappa (K) index, presented in the previous section, conditional Kappa index (k) (Congalton and Green, 1999) was used to assess the agreement between SLs maps and the published documents mentioned above. Conditional Kappa index (k) assess the agreement between individual categories of a pair of maps, being the following equation:

$$k_i = \frac{NX_{ii} - X_{i+} * X_{+i}}{NX_{i+} - X_{i+} * X_{+i}} \quad (4)$$

In this case, i represent shallow lake and no shallow lake classes. Conditional Kappa index allows to discriminate the influence of non shallow lakes class in the Overall Kappa index results.

3. Results

3.1. NDVI shallow lake water threshold

NDVI values of the cover types which dominate the study area are shown in Fig. 4. The mean NDVI values associated with shallow lakes ranged between −0.07 and 0.34 (A–E, Fig. 4), while non lake areas NDVI ranged between 0.57 and 0.68 (F–H, Fig. 4). Cover types

Table 2
Water level sets. Three periods were defined, each with four sets according to the water level ("wl") in relation to the mean water level of the period. The short name of the set and the number of images are indicated. The standard error ("SE") of the SL area calculation depends on the number of images and was estimated with a linear regression model adjusted after a sensitivity analysis. For more details, see Section 2.5.

Period	Years	Mean water level (cm)	Set	Water levels included (cm) ("wl")	Short name	No. of images	Estimated SD (%)
Complete	1987–2010	372	Total	All	CP total	77	0.0
			Low water	wl < 342	CP LWL	28	6.9
			Middle water	342 ⩾ wl > 402	CP MWL	15	25.3
			High water	wl ⩾ 402	CP HWL	34	0.0
WET	1987–1999	402	Total	All	WET total	42	0.0
			Low water	wl < 372	WET LWL	10	32.4
			Middle water	372 ⩾ wl > 432	WET MWL	15	25.3
			High water	wl ⩾ 432	WET HWL	17	22.5
DRY	2000–2010	320	Total	All	DRY total	35	0.0
			Low water	wl < 290	DRY LWL	12	29.6
			Middle water	290 ⩾ wl > 350	DRY MWL	11	31.0
			High water	wl ⩾ 350	DRY HWL	12	29.6

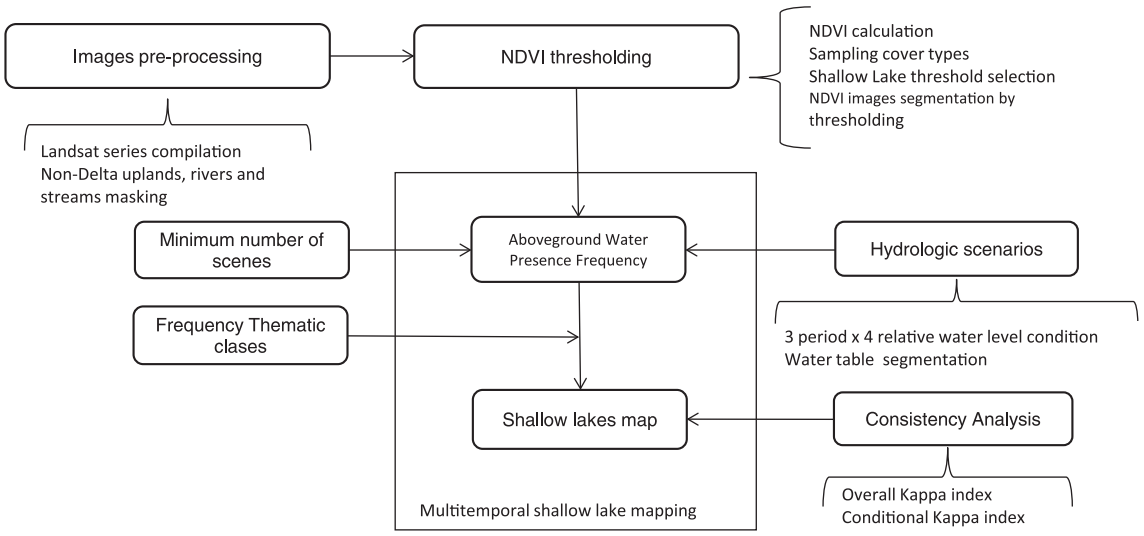

Fig. 3. Schematic diagram of the methodology.

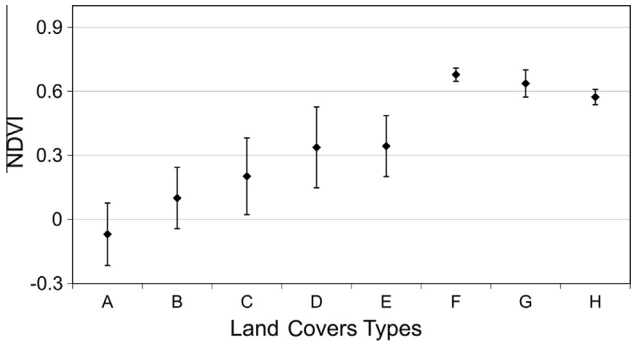

Fig. 4. NDVI for different cover types in the study area of the Paraná floodplain. A: water bodies with high content of suspended sediments, B: water bodies with high content of phytoplankton, C: water bodies dominated by submersed macrophytes, D: water bodies with emergent macrophytes, E: water bodies full covered with emergent and floating macrophytes, and Surrounding marshes, F: shrubland, G: short graminoids prairie, H: tall graminoids prairie.

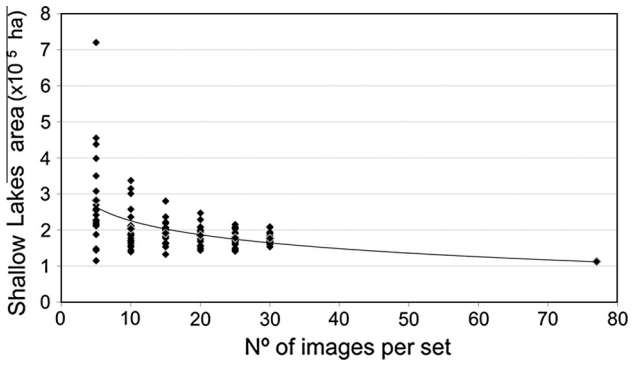

Fig. 5. Sensitivity analysis showing the reduction in the dispersion of the results. Each point represents the estimated shallow lakes coverage from randomly selected 5–30 images of the complete period.

A–E were significantly different from F–H ($p < 0.0001$). Since SL presence was considered not only for clear open water bodies but also for other cover types, the selected NDVI threshold considered the fuzzy influence of the macrophytes and thus minimized the loss of SL area mapped. According to these results, a NDVI threshold (T) was set in 0.34.

3.2. Minimum number of scenes

SL area differed according to the number of images in the set ($p = 0.0012$) (Fig. 5). The estimated standard deviation of the SL area ranged between 0 and 32.4% (mean = 16.9%). The standard deviation of the SL area decreased non-linearly with the number of images in the set ($p = 0.0154$, $R^2 = 0.8041$). If we considered a standard deviation of the area covered by shallow lakes lower than 10% the optimum number of images should be around 30 (SD = 8.8%), which is a rather high number of cloud free Landsat images to be available for any project. The SL area estimated with sets of 5 random dates significantly differed from that estimated with the sets of 10 or more images ($p < 0.001$), so a minimum of 10 image dates should be acceptable.

3.3. Effects under different hydrological scenarios

Fig. 6 shows the 12 SLs maps obtained under different hydrological scenarios. Shallow lakes are rather regularly spread all over the area as small dots between the main streams of the floodplain in this area: Paraná, Paraná Pavón and Victoria rivers (see Fig. 1 for their location). The total SL area depended on the hydrological conditions of the analyzed set (Fig. 7): 112,691 ha in CP-Total (10.9% of the study area), 65,754 ha in DRY-Total (6.4%) and 111,063 ha in WET-Total (10.7%). The SL area of the CP-Total was similar and slightly higher than the SL area of the WET-Total, in this case all the sets had more than 30 scenes (77 for CP-Total, 42 for 1987–1999 in the wet period, and 35 scenes for 2000–2010 during the dry period). As expected, the resulting SL area for each set of the WET period is always higher than the others, ranging from 10% to 26% of the study area.

The minimum SL area was found in DRY-LWL (59,227 ha; 5.7%) and the maximum in WET-HWL (271,538 ha 26.3%). The SL area increased with the relative water level (LWL < MWL < HWL) within a given period (CP, WET or DRY) (Fig. 7). For example, for the CP the SL area for the LWL set was 6% lower than for the MWL set, whereas the SL area for the HWL set was 20% higher than for the MWL set. However, the SL area remained stable around 65,000 ha in the DRY period (ca. 6% of the study area), with a slight

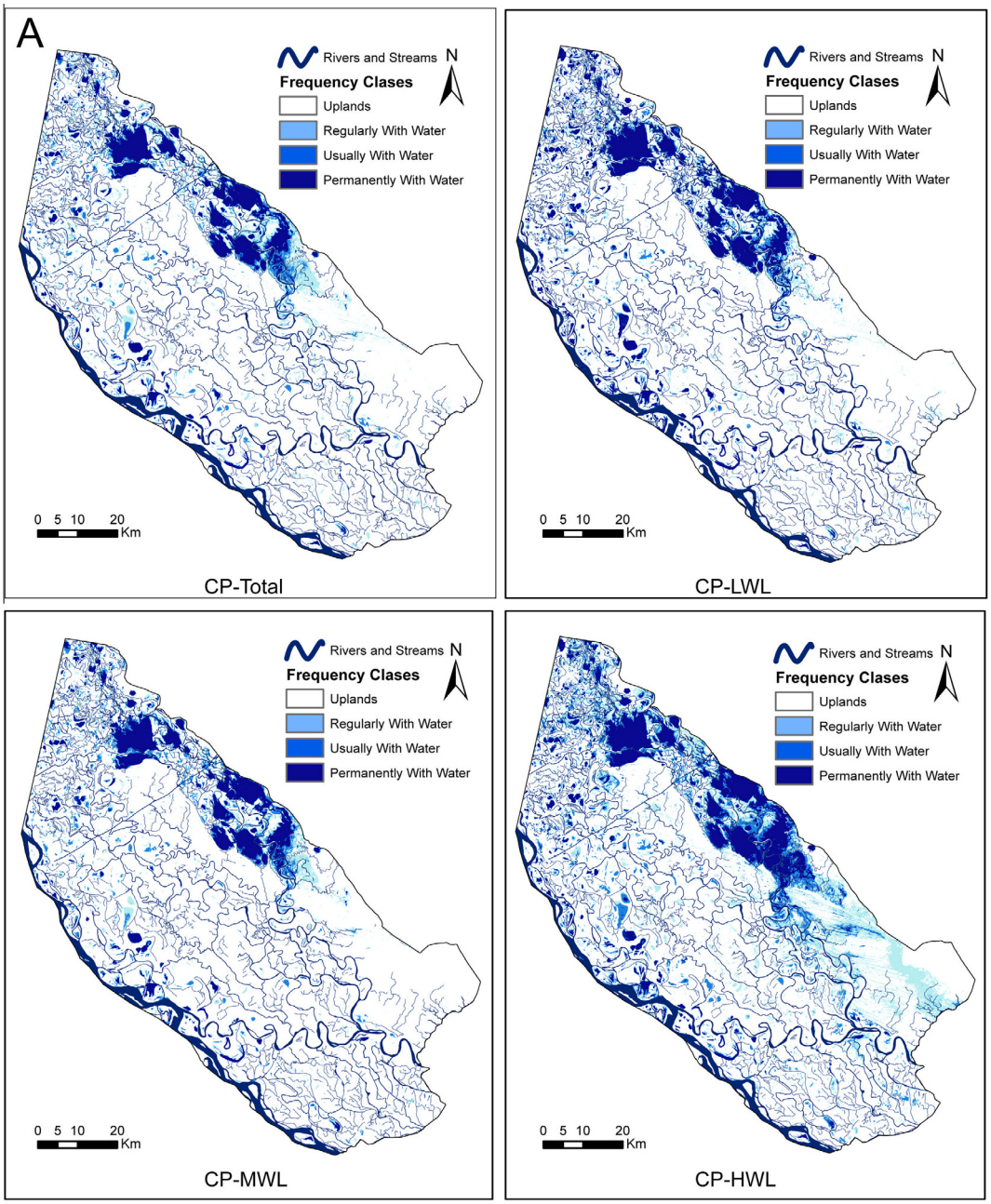

Fig. 6. Shallow lakes maps for twelve sets of images, classified in three flood frequency classes. (a) Sets of the Complete period (1987–2010). (b) Sets of the wet period (1987–1999). (c) Sets of the dry period (1999–2010).

increment (up to 8%) when the HWL set was used. The SL area from WET-MWL is higher than that for the WET-Total (18.4% and 10.7%, respectively), probably due to the weight of the non flooded images in the WET-Total set (Table 2).

When comparing SLs maps derived from Total sets, the highest similarity was found for CP and WET ($K = 95.86\%$); whereas the lowest similarity was found between WET and DRY ($K = 24.94\%$). For Middle levels (MWL sets), the highest similarity was found for CP and DRY-MWL ($K = 65.92\%$), while the lowest similarity was found for WET and DRY ($K = 35.18\%$) (Table 3).

The SL maps also differed according to the shallow lake water frequency classes. The class "Permanently with water" resulted relatively stable. Large permanent shallow lakes placed in the northern portion of the study area (Lakes around Victoria city) remain stable but change a lot in extension (Fig. 6). Analyzing results derived from Total sets again, Fig. 8a shows that "Permanently with water" class on the CP map covered 4.2% of the study area (38.5% of the SL area of the period), the class "usually with water" covered 2.2% (20.2% of the SL area of the period) and the class "regularly with water" 4.5% (41.3% of the SL area of the period). In this figure we can also see that these values remained almost the same for the WET set, in accordance with the fact that the total area of SL is similar for both maps. On the contrary, the pattern is totally different for the DRY period, remaining the area of "permanent with water" class similar to the other sets but having a decrease in usually and regularly categories.

Fig. 8b presents shallow lake water frequency classes distribution for MWL sets (CP, Wet and DRY) which have a similar number of images (15, 15 and 11 respectively), and represents subsets of the Total sets which consider only middle water level situations

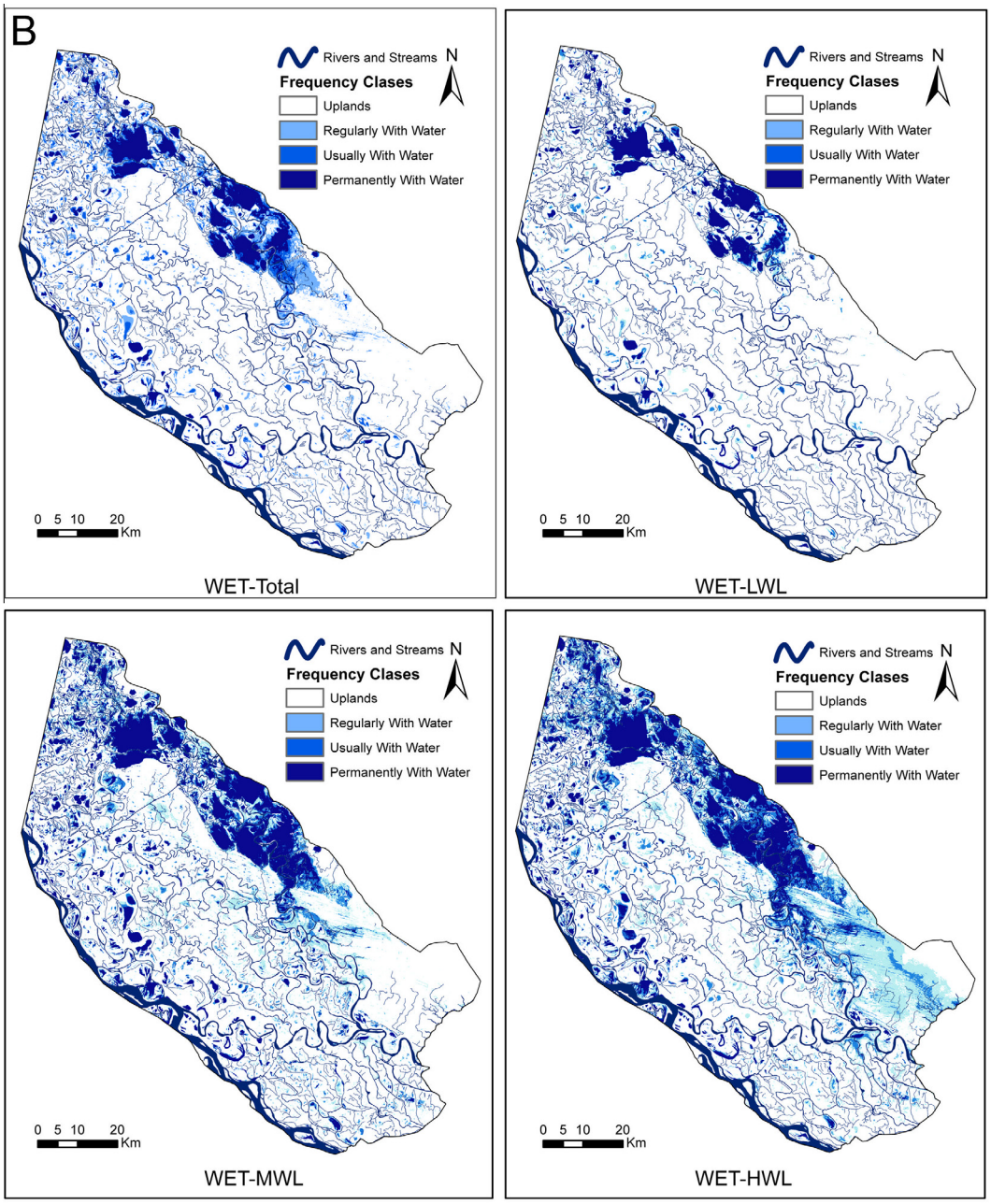

Fig. 6 (*continued*)

around the mean. Distribution patterns of the areas of the frequency classes strongly differ between MWL sets. The pattern and total area of the DRY-MWL is similar to those of DRY-Total results (Fig. 8a), but CP and WET patterns differ under MWL conditions and compared to Total sets.

3.4. Comparisons with previous shallow lakes maps

The comparison between the SLs map obtained with the DRY-LWL set and the maps made by Borro et al. (2010a) resulted in an overall Kappa index of 49%. The comparison between the SLs map obtained with the CP-Total set and the maps made by Borro et al. (2010b) showed an overall Kappa index of 78.39%.

Regarding the comparisons between our SLs maps and the SIG250 database, the overall Kappa index values were always less than 52% and the conditional Kappa index values (considering water and non water classes) were always less than 20% (Table 4). The comparisons between our SLs maps and the SRTM lakes and wetlands database, always resulted in overall Kappa indexes values greater than 70% (Table 4): the highest values were obtained for the comparisons with DRY-LWL and CP-LWL sets.

4. Discussion

One of the main features of the South America river floodplains, and particularly of the Paraná River is the large number of shallow lakes, highly variables in size, shape and water permanency (Drago, 2007). Shallow lakes (SL) are a special case of lakes, and their definition needs to be pragmatically adapted to the features of the study area following an ecological basis (Padisák and Reynolds, 2003). Our approach involved a frequency analysis based on a time series of NDVI derived from historical optical Landsat TM

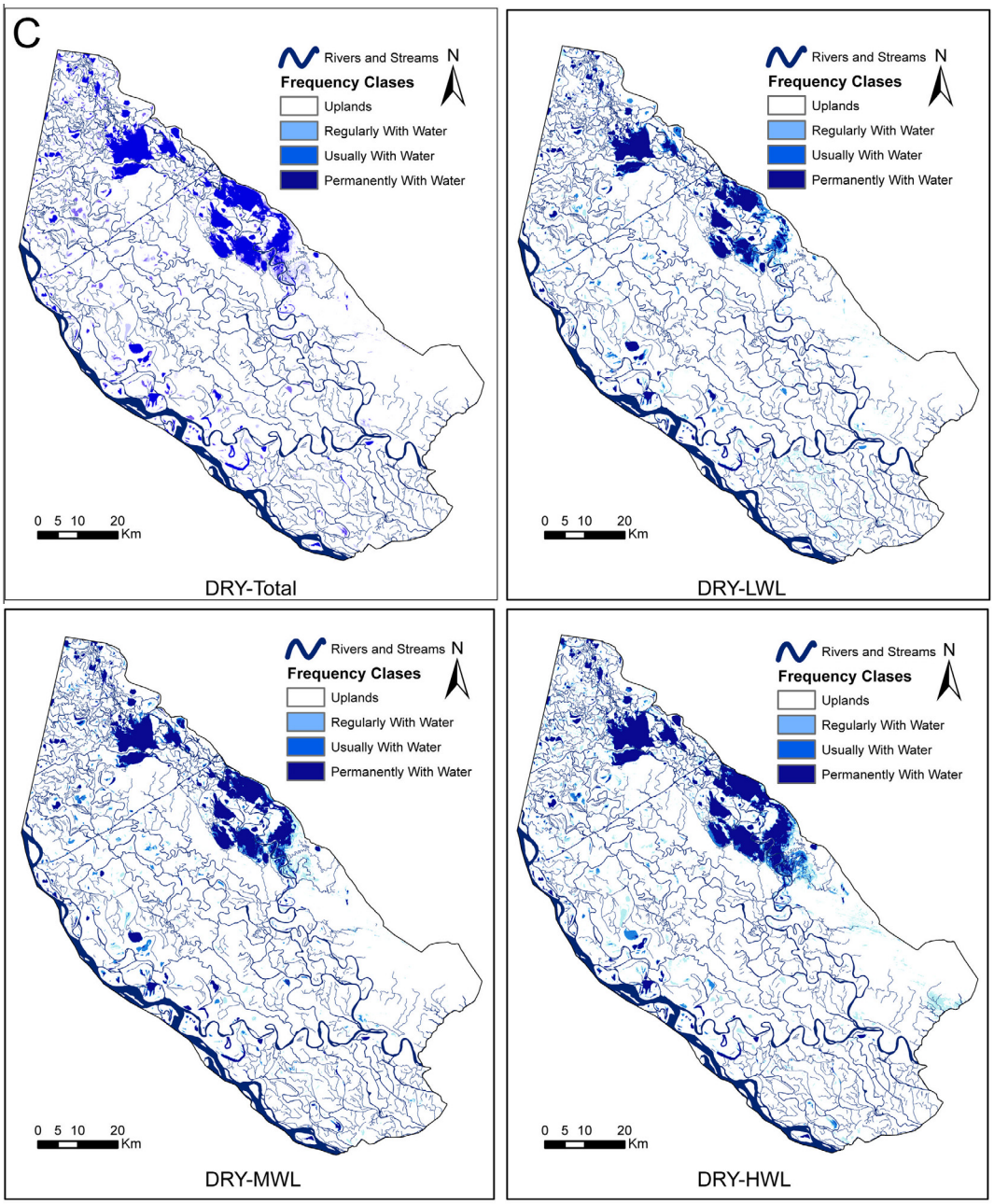

Fig. 6 (*continued*)

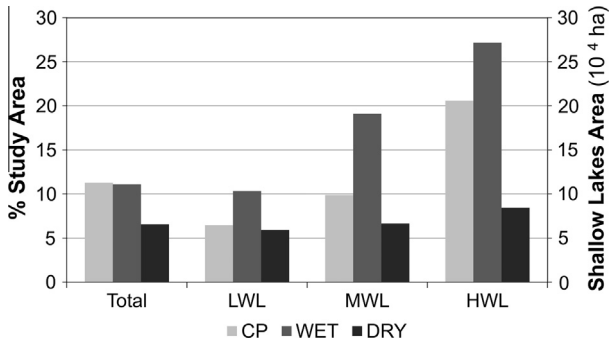

Fig. 7. Area of shallow lakes computed for the 25 twelve sets belonging to the combinations of periods (CP, WET, DRY) and water level sets (Total, Low, Middle, High). For details on the definition of the sets, see Table 1.

imagery. The results showed that SL can be accurately defined with this methodology, reducing the uncertainties of the fuzzy boundaries between SL and their surrounding marshes. In addition, the analysis of sets of images belonging to different hydrological conditions allowed us to show the variability of the SL area, the SL types (permanently with water, usually with water, regularly with water) and its spatial distribution in the floodplain. Since the selected NDVI threshold was greater than 0, it also included alternate clear and turbid states and SL covered by macrophytes (Scheffer et al., 2001). Likewise, it also includes mixed pixels covered by different fractions of water and vegetation (Malthus and George, 1997). Although this positive value may overestimate the area of SL, frequency analysis helps excluding pixels of wetlands that only eventually have water coverage but are not a SL. Nevertheless, underestimations of SL area may occur in areas always covered

Table 3
Comparisons between shallow lakes maps obtained for different hydrological conditions. Overall Kappa evaluated changes in the map as a whole. Pairs with Kappa values near to 100% have high similarity; pairs with Kappa values near to 0% have low similarity.

	CP-total	CP-HWL	CP-MWL	CP-LWL	WET-total	WET-HWL	WET-MWL	WET-LWL	DRY-total	DRY-HWL	DRY-MWL	DRY-LWL
CP-Total	100.00	47.4	81.98	57.04	95.86	34.05	45.4	69.87	59.1	64.68	60.99	46.96
CP-HWL		100.00	45.49	32.09	46.5	65.52	67.8	52.09	32.96	40.15	33.95	26.54
CP-MWL			100.00	61.82	83.1	32.36	43.29	68.88	64.46	65.33	65.92	50.8
CP-LWL				100.00	57.85	24.11	33.06	52.84	81.58	64.77	75.62	51.35
WET-Total					100.00	33.55	44.75	63.9	59.9	65.5	61.8	47.5
WET-HWL						100.00	58.26	40.6	24.94	30.19	25.69	19.83
WET-MWL							100.00	53.96	34.15	39.84	35.18	50.8
WET-LWL								100.00	53.8	54.79	54.21	44.28
DRY-Total									100.00	70.3	84.7	69.8
DRY-HWL										100.00	69.34	55.38
DRY-MWL											100.00	65.87
DRY-LWL												100.00

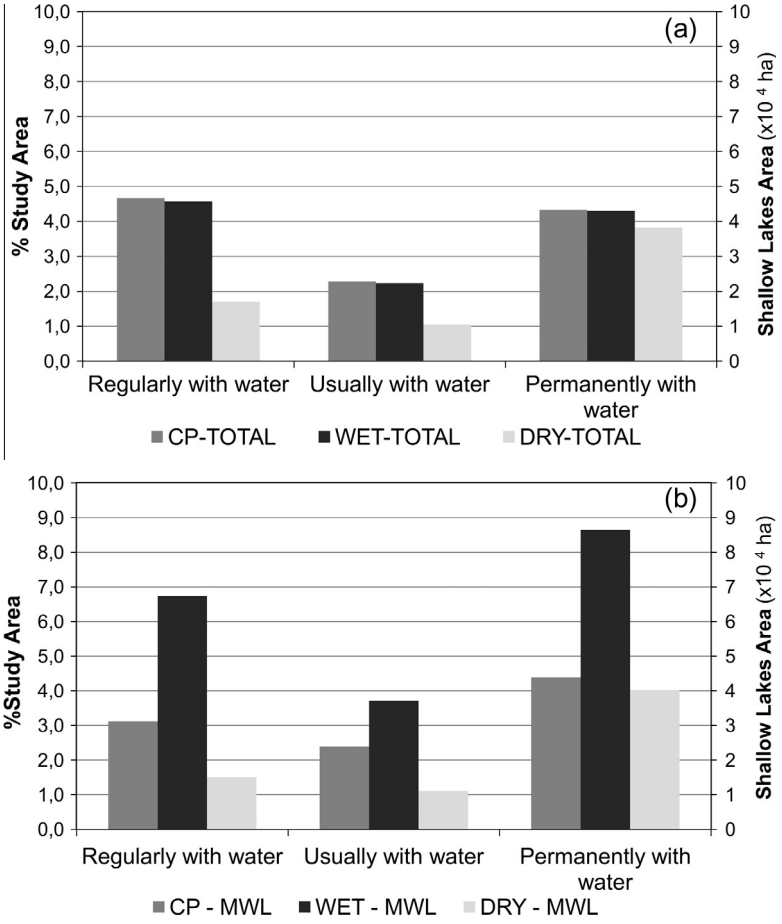

Fig. 8. Area of flooding classes in shallow lakes reported as percentage of the study area (left axis) and hectares (right axis) for different sets. (a) Total sets and (b) middle water Level (MWL) sets.

by macrophytes that can have such a strong signal as to prevent the water below them to be detected (Jakubauskas et al., 2000).

Frequency analysis includes a temporal dimension that is not usually addressed in SL mapping. At most cases, approaches are based on the comparison of few satellite images under high and low water states using radar (Hess et al., 2003) or optical sensors (Frazier et al., 2003; Ordoyne and Friedl, 2008). Our results show that the number of analyzed images has a strong influence on the estimated shallow lake area (Fig. 5). If the analysis includes only few images, the variability of the shallow lakes area of the floodplain in each image produces a large uncertainty. The number of images involved in a multitemporal frequency analysis is critical: a very low number of images might estimate the SL area with a high standard deviation, whereas a very high number of images might lead to an excessive processing time without substantially improving the precision of the results obtained. As the number of analyzed images increases, a stabilization of the estimated SL area occurs, and in our case, the optimum number of images was 30.

Thus, the area defined as SL with a single scene approach will vary according to the particular moment of each image acquisition. Using 30 images, SL area ranged between 153,600 ha and 209,000 ha; whereas using only five images SL ranged between 115,000 ha and 720,000 ha. The inclusion of the temporal dimension allows overcoming the particular state of each image. Thus,

Table 4
Summary of the Overall Kappa index and conditional Kappa index for the three periods in comparison with the two Shallow Lakes data bases SIG 250 and SRTM.

Short name of the set	SIG 250		SRTM	
	Overall Kappa	Conditional Kappa	Overall Kappa	Conditional Kappa
CP_Total	46.54	8.96	87.38	86.35
CP_HWL	49.50	15.92	78.14	92.21
CP_MWL	45.66	7.55	88.48	81.15
CP_LWL	44.28	4.85	92.32	78.78
WET_Total	46.45	8.80	87.54	86.29
WET_HWL	50.50	19.68	72.73	91.82
WET_MWL	51.03	16.79	79.47	93.85
WET_LWL	46.70	9.41	86.58	86.44
DRY_Total	44.23	4.86	92.11	77.97
DRY_HWL	44.88	6.21	89.87	77.38
DRY_MWL	44.25	4.90	92.12	79.01
DRY_LWL	44.08	4.40	92.85	75.96

it improves the probability of detection of permanent SL: it is possible to acquire images where the water surface is exposed due to vegetation disappearance (burning, drought, displacement or flooding). In addition, temporal series allow the detection of temporary water bodies that in a single image may be mistaken with surrounding areas (uplands or surrounding marshes).

There is relatively good agreement between our resulting SL (CP-Total) map and Borro et al. (2010b) but substantial differences exist between SL map (DRY-LWL) and Borro et al. (2010a). In the first one, the relative large number of images used in Borro et al. (2010b), contribute to a better identification of the SL. In the second case, we have no doubt that having only one image may produce a large distortion on the SL mapping. The SL area obtained from the complete set of images is much higher than the area mapped in the SIG 250, which is the official cartography of Argentina ($K < 52\%$, $k < 20\%$, Table 4). The difference between SIG250 and our results corresponds mainly to the fact that SIG250 only includes the permanent lagoons of the floodplain, not considering temporal shallow lakes and fluctuating peripheral areas of the permanent water bodies. Regarding the SRTM lakes and wetlands database, our results show a much better agreement than with SIG250 ($K > 72\%$, $k > 75\%$). However, there are subtle differences between the maps from different sets, due to the influence of hydrometric conditions on the estimated area of lagoons.

The total area of SL is highly influenced by the hydrological state of the analyzed period, and by the hydrometric situation of the set of images considered (Figs. 6 and 7). However, the area of the "permanently with water" SL class remains relatively stable among the complete stacks regardless of the period (Figs. 6a and 8a). These lakes occupy nearly 40,000 ha, from which 32,000 ha correspond to permanent lakes of large extension (between 1000 and 8000 ha) like those next to the cities of Victoria and Ramallo (Figs. 1 and 6). The classes "usually with water" and "regularly with water" are dotted within the study area as small water bodies or as borders of permanent water bodies (Fig. 6).

Differences in the SL area and water frequency classes obtained between MWL and Total sets, are interesting not only because they may illustrate the importance of the number of images involved in the analysis, but they also may suggest the influence of extreme water level conditions represented in the datasets (Fig. 8). In this way, results are very sensitive not only to the number of images but to the hydrological condition on their acquisition date.

The identification of the non permanent SL is important since their total area is much larger than the permanent SL area. This implies that if we only consider the permanent water bodies of a region, like in SIG250, we are strongly underestimating the water offer of the region. This becomes extremely important when the aim is the study of the water cycle, hydrological modeling, evapotranspiration patterns, and water offer for models of productive activities. In this sense, our results in a floodplain agree with the global view of Downing (2010): the SL should be considered with much attention because they are more numerous worldwide than deep lakes, providing humankind with many services such as nutrition, water for drinking, irrigation and dilution of pollutants, transportation, recreation and aesthetic enjoyment.

In contrast with temperate developed countries, the wetlands of South American temperate zones still maintain a high degree of conservation (Brinson and Malvárez, 2002). Nevertheless, during the last decades the largest river basins of the continent are highly threatened by hydrological regulation engineering constructions (for energy supply, farming developments, and roads) that change the hydrological regime. As has been widely reported, changes in the hydrological balance strongly affect the existence and spatial extension of wetlands and SL which may be consider as sensitive hydrological indicators (Hudson et al., 2012; Neiff and Iriondo, 1994; Wolski and Savenije, 2006).

Finally, Landsat images time series provide an accurate spatial and temporal resolution for SL identification in floodplains, particularly in temperate zones where there is a good provision of cloud free images. The Landsat Program is a unique series of Earth-observing satellite missions that acquires data from the Earth's surface since 1972 and acquires data steadily and systematically since 1985 (Landsat 5 and Landsat 7 + ETM). The recent launch of Landsat 8 satellite guarantees the continuity of the mission and will generate a unique data set that will surely facilitate the development of monitoring programs for terrestrial natural resources. Concordantly, the use of the method proposed and evaluated in this paper resulted in a robust database of shallow lakes for the studied area of the Paraná floodplain and their temporal behavior that could be useful to establish monitoring programs related to the impact of climate and man made changes at landscape scale.

Acknowledgements

This research was funded by Agencia Nacional de Promoción Científica y Técnica (PICT 1849/06, PICTO CIN I 0022, Argentina). María Marta Borro and Natalia Soledad Morandeira have a Postgraduate Fellowship of the Consejo Nacional de Investigaciones Científicas y Técnicas (Argentina). We wish to thank Carlos Ramonell and Ing. I. Cristina, from Centro de Informaciones Meteorológicas de la Universidad Nacional del Litoral (CIM – UNL) for providing water level records. We also thank the three anonymous reviewers for their comments and suggestions on a previous draft of this manuscript. Great part of the field work was carried out at ranches owned by Juan Nazar and Abel Matera. The settlers Ernesto, Luis Bello and his family were very helpful and kindness. Facundo Schivo, Carolina Hernando, Fabricio Baronetti, Sol Varela and Martín Schoo helped with field work.

References

Baigún, C.R.M., Puig, A., Minotti, P.G., Kandus, P., Quintana, R., Vicari, R., Bo, R., Oldani, N.O., Nestler, J.A., 2008. Resource use in the Parana River Delta (Argentina): moving away from an ecohydrological approach? Ecohydrol. Hydrobiol. 8 (2–4), 245–262.

Bó, R.F., Quintana, R.D., 1999. Actividades humanas y biodiversidad en humedales: el caso del Bajo Delta del río Paraná. 291–316. In: Matteucci, S.D., Solbrig, O.T., Morello, J.H., Halffter, G. (Eds.), Biodiversidad y Uso de la Tierra. EUDEBA, Colección CEA (24): 1–580.

Borro, M.M., Morandeira, N.S., Salvia, M.M., Minotti, P.G., Puig, A., Karszenbaum, H., Kandus, P., 2010a. "Las lagunas de la planicie aluvial del Delta del Río Paraná: clasificación multitemporal e integración con datos limnológicos". In: Hacia la gestión integral de los recursos hídricos en zonas de llanuras. Varni, M., Entraigas, I. y Vives, L. (Eds.). Libro de Actas del 1 Congreso Internacional de Hidrología de Llanuras, Azul, Buenos Aires, Argentina. 639–646, ISBN: 978-987-543-393-9 Pp.

Borro, M.M., Salvia, M., Minotti, P.G, Puig, A., Karszenbaum, H., Kandus, P., 2010b. Primeros resultados de la clasificación de lagunas someras en la Región del Delta del Paraná bajo un enfoque eco-hidrogeomórfico In: Cambios de uso de la tierra Causas, consecuencias y mitigación. Menghi, M y Matteucci, S.D. (Eds). Buenos Aires. Asociación Argentina de Ecología de Paisaje. ISBN 978-987-33-0213-8. Pp. 27–34. <http://www.asadep.org.ar/LibrolIjaep/Borro.pdf>.

Brinson, M.M., Malvárez, A.I., 2002. Temperate freshwater wetlands: types, status, and threats. Environ. Conserv. 29, 115–133.

Caccamo, G., Chisholm, L.A., Bradstock, R.A., Puotinen, M.L., 2011. Assesing the sensitivity of MODIS to monitor drought in high biomass ecosystems. Remote Sens. Environ. 115 (10), 2626–2639.

Carignan, R., Neiff, J.J., 1992. Nutrient dynamics in the floodplain ponds of the Paraná River (Argentina) dominated by the wáter hyacinth *Eichornia crassipes*. Biogeochemistry 17, 85–121.

Congalton, R.G., Green, K., 1999. Assessing the Accuracy of Remotely Sensed Data: Principles and Practices. CRC/Lewis Publishers, Boca Raton, USA, ISBN 0-87371-986-7.

Cowardin, L.M., Peterson, S.A., 1997. Introduction. In: Peterson, S.A., Carpenter, L., Guntenspergen, G., Cowardin, L.M. (Eds.). Pilot Test of Wetland Condition Indicators in the Prairie Pothole Region of the United States, EPA/620/R-97/002, pp. 1–9.

Cózar, A., García, C.M., Gálvez, J.A., Loiselle, S.A., Bracchini, L., Cognetta, A., 2005. Remote sensing imagery analysis of the lacustrine system of Ibera wetland (Argentina), Ecol. Model., 186(1), 29–41. ISSN: 0304-3800, doi: http://dx.doi.org/10.1016/j.ecolmodel.2005.01.029.

Crist, E.P., Cicone, R.C., 1984. A physically-based transformation of Thematic Maper data – the TM Tasseled Cap. IEEE Trans. Geosci. Remote Sens. 22 (3), 256–263.

De Jager, N.R., Rohweder, J.J., 2012. Spatial patterns of aquatic habitat richness in the Upper Mississippi River floodplain, USA. Ecol. Indic. 13, 275–283.

Downing, J.A., 2010. Emerging global role of small lakes and ponds: little things mean a lot. Limnetica 29 (1), 9–24.

Drago, E.C., 2007. The physical dynamics of the river–lake floodplain system. In: Iriondo, M.H., Paggi, J.C., Parma, M.J. (Eds.), The middle Paraná river: limnology of a subtropical wetland. Springer-Verlag, Berlin, Alemania, pp. 83–122.

Feng, L., Hu, C., Chen, X., Cai, X., Tian, L., Gan, W., 2012. Assesment of inundation changes of Poyang Lake using MODIS observations between 2000 and 2010. Remote Sens. Environ. 121, 80–92.

Frazier, P., Page, K., Louis, J., Briggs, S., Robertson, A.I., 2003. Relatin wetland inundation to river flow using Landsat TM data. Int. J. Remote Sens. 24 (19), 3755–3770.

Gao, B.C., 1996. NDWI a normalized difference water index for remote sensing of vegetation liquid water from space. Remote Sens. Environ. 58, 257–266.

Hardisky, M.A., Klemas, V., Smart, R.M., 1983. The influence of soft salinity, growth form, mad leaf moisture on the spectral reflectance of *Spartina alterniflora* canopies. Photogram. Eng. Remote Sens. 49, 77–83.

Hess, L.L., Melack, J.M., Novo, E., Barbosa, C.C.F., Gastil, M., 2003. Dual-season mapping of wetland inundation and vegetation for the central Amazon Basin. Remote Sens. Environ. 87 (4), 404–428.

Hudson, P.F., Heitmuller, F.T., Leitch, M.B., 2012. Hydrologic connectivity of oxbow lakes along the lower Guadalupe River, Texas: the influence of geomorphic and climatic controls on the "flood pulse concept". J. Hydrol. 414–415, 174–183.

Instituto Geográfico Nacional, 2001. SIG 250. <http://www.ign.gob.ar/sig250> and <http://www.ign.gob.ar/archivos/sig250/publicacion-conae-2012/004_Cuerpos_De_Agua.zip>.

Iriondo, M.H., 1988. A comparison between the Amazon and Paraná river systems. Mitt. Geol. Palaont. Inst. Univ. Hamburg SCOPE/UNEP Sonderbd 66, 77–92.

Iriondo, M., Scotta, E., 1979. The evolution of the Paraná River Delta. In: Proceedings of the 1978 International Symposium on Coastal Evolution in the Quaternary, September 11–18, 1978, SaoPaulo, 405–418pp.

Jakubauskas, M., Kindscher, K., Fraser, A., Debinski, D., Price, K.P., 2000. Close-range remote sensing of aquatic macrophyte vegetation cover. Int. J. Remote Sens. 21 (18), 3533–3538. http://dx.doi.org/10.1080/014311600750037543.

Junk, W.J., Bayley, P.B., Sparks, R.E., 1989. The flood pulse concept in river–floodplain systems. In: Dodge, D., (Ed.), Proceedings of the International Large River Symposium (LARS). Can. Spec. Pub. Fish. Aquat. Sci. 106, 110–127.

Kandus, P., Malvárez, A.I., Madanes, N., 2003. Estudio de las comunidades de plantas herbáceas de las islas bonaerenses del Bajo Delta del Río Paraná (Argentina). Darwiniana 41, 1–16.

Keddy, P.A., 2010. Wetland Ecology Principles and Conservation. Cambridge University Press, Cambridge, UK, ISBN 978-0-521-73967-2.

Kloiber, S., Brezonik, P., Bauer, M., 2002. Application of Landsat imagery to regional-scale assessments of lake clarity. Water Res. 36 (17), 4330–4340.

Landis, J.R., Koch, G.G., 1977. The measurement of observer agreement for categorical data. Biometrics 33, 159–174.

Latrubesse, E.M., Stevaux, J.C., Sinha, R., 2005. Tropical rivers. Geomorphology 70, 187–206.

Malthus, T.J., George, D.G., 1997. Airborne remote sensing of macrophytes in Cefni Reservoir, Anglesey, UK. Aquat. Bot. 58, 317–332.

Malvárez, A.I., 1997. Las comunidades vegetales del Delta del Río Paraná. Su relación con factores ambientales y patrones de paisaje, Ph.D. Thesis, Facultad de Ciencias Exactas y Naturales, Universidad de Buenos Aires.

Mertes, L.A.K., Novo, E.M.L., Daniel, D.L., Shimabukuro, Y.E., Richey, J.E., Krug, T., 1996. Classification of Rios Solimoes-Amazonas wetlands through application of spectral mixture analysis to landsat thematic mapper data. In: VIII Simposio Brasileiro de Sensoriamento Remoto, Salvador-Brazil, 1996.

Morandeira, N., Gramuglia, P., Salvia, M., Madanes, N., Vicari, R., Minotti, P.G., Quintana, R.D., Karszenbaum, H., Kandus, P., 2011. Vegetación, in: Kandus, P., Minotti, P.G., Borro, M.M. (Eds.). Contribuciones al conocimiento de los humedales del Delta del Río Paraná. Herramientas para la evaluación de la sustentabilidad ambiental. PICT 1849, ANPCyT MINCyT. 30pp. ISBN: 978-987-1435-35-7.

Neiff, J.J., 1990. Ideas para la interpretación ecológica del Paraná. Interciencia 15 (6), 424–441.

Neiff, J.J., Iriondo, M.H., Carignan, R., 1994. Large tropical South American wetlands: an overview. In: Link, G.L., Naiman, R.J. (Eds.), The Ecology and Management of Aquatic-terrestrial Ecotones. Proceedings Book, Univ. of Washington, pp. 156–165.

Olmanson, L.G., Bauer, M.E., Brezonik, P.L., 2008. A 20-year Landsat water clarity census of Minnesota's 10,000 lakes. Remote Sens. Environ. 112 (11), 4086–4097.

Ordoyne, C., Friedl, M.A., 2008. Using MODIS data to characterize seasonal inundation patterns in the Florida Evergaldes. Remote Sens. Environ. 112 (11), 4107–4119.

Ozesmi, S.L., Bauer, M.E., 2002. Satellite remote sensing of wetlands. Wet. Ecol. Manage. 10, 381–402.

Padisák, J., Reynolds, C., 2003. Shallow lakes: the absolute, the relative, the functional and the pragmatic. Hydrobiologia 506 (509), 1–11.

Peng, D.Z., Xiong, L.H., Guo, S.L., Shu, N., 2005. Study of Dongting Lake area variation and its influence on water level using MODIS data. Hydrolog. Sci. J. 50 (1), 31–44.

Poi de Neiff, A., Neiff, J.J., 2006. Riqueza de especies y similaridad de los invertebrados que viven en plantas flotantes de la planicie de inundación del río Paraná. Interciencia 31 (3), 220–225.

Prefectura Naval Argentina <http://www.prefecturanaval.gov.ar/web/es/html/dico_alturas.php>.

Quintana, R.D., Madanes, N., Malvárez, A.I., Kalesnik, F.A., 2005. Análisis de la vegetación en tres tipos de hábitat de Carpinchos en la baja cuenca del Río Paraná, Argentina. Serie Misc. INSUGEO 14, 183–200.

Quirós, R., Cuch, S., 1989. The fisheries and limnology of the lower Plata Basin. In: Dodge, D.P (Ed.), Proceedings of the International Large River Symposium. Can. Spec. Publ. Fish. Aquat. Sci. 106, 429–443.

R Core Team, 2012. R: A Language and Environment for Statistical Computing. R Foundation for Statistical Computing, Vienna, Austria, ISBN 3-900051-07-0, <http://www.R-project.org/>.

Rabus, B., Eineder, M., Roth, A., Bamber, R., 2003. The shuttle radar topography mission – a new class of digital elevation models acquired by spaceborne radar. ISPRS J. Photogramm. Remote Sens. 57 (4), 241–262.

Ritchie, J.C., Zimba, P.V., Everitt, J.H., 2003. Remote sensing techniques to assess water quality. Photogramm. Eng. Rem. S. 69 (6), 695–704.

Satterhwaite, F.E., 1941. Synthesis of variance. Psychometrika 6 (5), 309–316.

Scheffer, M., 1998. Ecology of Shallow Lakes. Chapman and Hall, London.

Scheffer, M., Carpenter, S., Foley, J.A., Folke, C., Walker, B., 2001. Catastrophic shifts in ecosystems. Nature 413, 591–596.

Sendacz, S., 2001. Planktonic Copepoda of the Upper Paraná River floodplain lakes (Sao Paulo and Mato Grosso do Sul, Brazil). Hydrobiologia 453–454 (1), 367–374.

Silva, T.S.F., Costa, M.P.F., Melack, J.M., Novo, E.M.L.M., 2008. Remote sensing of aquatic vegetation: theory and applications. Environ. Monit. Assess. 140, 131–145. http://dx.doi.org/10.1007/s10661-007-9855-3.

Stein, A., 2008. Handling uncertainties in image mining for remote sensing studies. In: Proceedings of the 8th International Symposium on Spatial Accuracy Assessment in Natural Resources and Environmental Sciences Shanghai, P.R. China, June 25–27, 2008, pp. 362–368.

Stumpf, R.P., 1992, Remote sensing of water clarity and suspended sediments in coastal waters: needs and solutions for pollution monitoring, control, and abatement, In: Proceedings First Thematic Conference on Remote Sensing for

Marine and Coastal Environments, (SPIE 1930), ERIM, Ann Arbor Michigan, pp. 293–305.
Tucker, C.J., 1979. Red and photographic infrared linear combinations for monitoring vegetation. Remote Sens. Environ. 8, 127–150.
Weiss, D., Crabtree, R.L., 2011. Percent surface water estimation from MODIS BRDF 16-day image composites. Remote Sens. Environ. 115, 2035–2046.
Wolski, P., Savenije, H.H.G., 2006. Dynamics of floodplain-island groundwater flow in the Okavango Delta, Botswana. J. Hydrol., 320(3–4), 283–301. ISSN 0022-1694.
Zhao, X., Stein, A., Chen, X.L., 2011. Monitoring the dynamics of wetland inundation by random sets on multi-temporal images. Remote Sens. Environ. 115 (9), 2390–2401. http://dx.doi.org/10.1016/j.rse.2011.05.002.